Relationship between Molecular Association and Re-entrant Phenomena in Polar Calamitic Liquid Crystals

ARTICLE *in* THE JOURNAL OF PHYSICAL CHEMISTRY B · JANUARY 2015

Impact Factor: 3.3 · DOI: 10.1021/jp512093j · Source: PubMed

THE JOURNAL OF PHYSICAL CHEMISTRY B

Article

pubs.acs.org/JPCB

Relationship between Molecular Association and Re-entrant Phenomena in Polar Calamitic Liquid Crystals

Richard J. Mandle,*[,†] Stephen J. Cowling,[†] Ian Sage,[‡] M. Eamon Colclough,[§] and John W. Goodby[†]

[†]Department of Chemistry, The University of York, York YO10 5DD, U.K.

[‡]Nottingham Trent University, Nottingham NG1 4BU, U.K.

[§]QinetiQ Ltd, Fort Halstead, Sevenoaks TN14 7BP, U.K.

Supporting Information

ABSTRACT: The relationship between molecular association and re-entrant phase behavior in polar calamitic liquid crystals has been explored in two families of materials: the 4′-alkoxy-4-cyanobiphenyls (6OCB and 8OCB) and the 4′-alkoxy-4-nitrobiphenyls. Although re-entrant nematic phase behavior has previously been observed in the phase diagram of 6OCB/8OCB, this is not observed in mixtures of the analogous nitro materials. As there is no stabilization of the smectic A phase in mixture studies, it was conjectured that the degree of association for the nitro systems is greater than that for the cyano analogues. This hypothesis was tested by using measured dielectric anisotropies and computed molecular properties to obtain a value of the Kirkwood factor, *g*, which describes the degree of association of dipoles in a liquid. These computed values of *g* confirm that the degree of association for nitro materials is greater than that for cyano and offer a useful method for quantifying molecular association in systems exhibiting a re-entrant polymorphism.

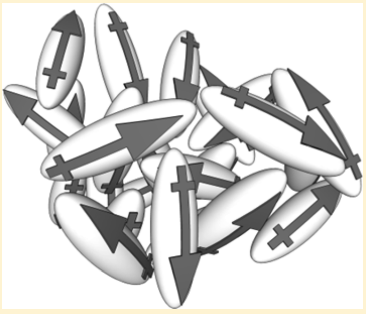

1. INTRODUCTION

Maier−Meier theory is used to describe the relationship between the molecular properties of a material to its bulk liquid crystalline properties.[1] The Maier−Meier relationship is effectively an extension of the Onsager theory of isotropic liquids to anisotropic liquids such as liquid crystals.[2] Specifically, it relates the molecular parameters of a compound to its bulk liquid crystalline properties, specifically the molecular polarizability ($\bar{\alpha}$ and $\Delta\alpha$), *effective* molecular dipole moment (μ_{eff}), and the angle between the dipole moment vector and the molecular long axis (β) with the bulk dielectric anisotropy ($\Delta\varepsilon = \varepsilon_{\parallel} - \varepsilon_{\perp}$), reaction field vectors ($\mathbf{F}$ and $\mathbf{h}$) and the order parameter (S), through eqs 1−3.[3,4] Typically, molecular properties are computed via semiempirical or quantum mechanical methods;[5−9] however, the accuracy of such methods must be ascertained by comparison with measured values, where available.

$$\varepsilon_{\parallel} = 1 + \frac{NFh}{\varepsilon_0}\left\{\bar{\alpha} - \frac{2}{3}\Delta\alpha S + \frac{F\mu_{\mathrm{eff}}^{\,2}}{3k_{\mathrm{B}}T}[1 - (1 - 3\cos^2\beta)S]\right\} \quad (1)$$

$$\varepsilon_{\perp} = 1 + \frac{NFh}{\varepsilon_0}\left\{\bar{\alpha} - \frac{1}{3}\Delta\alpha S + \frac{F\mu_{\mathrm{eff}}^{\,2}}{3k_{\mathrm{B}}T}\left[1 + \frac{1}{2}(1 - 3\cos^2\beta)S\right]\right\} \quad (2)$$

$$\Delta\varepsilon = \varepsilon_{\parallel} - \varepsilon_{\perp} = \frac{NFh}{\varepsilon_0}\left\{\Delta\alpha - \frac{F\mu_{\mathrm{eff}}^{\,2}}{2k_{\mathrm{B}}T}(1 - (3\cos^2\beta)\right\}S \quad (3)$$

As polar materials will tend to align antiparallel to minimize the net dipole of the bulk system, the Kirkwood factor (g) is used to reflect the degree of correlation.[10,11] The relationship between the molecular dipole moment (μ), the effective molecular dipole moment (μ_{eff}) and the Kirkwood factor (g) is given by

$$\mu_{\mathrm{eff}}^{\,2} = \mu^2 g \quad (4)$$

The Kirkwood factor has been used successfully to account for aggregation of polar solvents[12] as well as highly polar and ionic additives in nematic solutions.[6,13] A schematic representation of the relative alignment of two polar, rodlike molecules for Kirkwood factors of g = 0 and g = 2 is given in Figure 1.

Re-entrant behavior in liquid crystals is now an established phenomenon, over 39 years since the first observation of a re-entrant nematic phase in 1975 by Cladis.[14,15] Re-entrant behavior is not confined to soft mater, with re-entrant superconductivity having been also observed at the superconducting−ferromagnetic phase transition.[16] In a classical example of re-entrant behavior in liquid crystals, binary mixtures of 4-hexyloxy-4′-cyanobiphenyl (6OCB) and 4-octyloxy-4′-cyanobiphenyl (8OCB) exhibit a re-entrant nematic phase when the concentration of 6OCB is in the range of 20−30%.[17] The incidence of re-entrancy in materials with large longitudinal dipole moments, such as the 4-alkoxy-4′-cyano-

Received: December 4, 2014
Revised: January 20, 2015
Published: January 20, 2015

DOI: 10.1021/jp512093j
J. Phys. Chem. B 2015, 119, 3273−3280

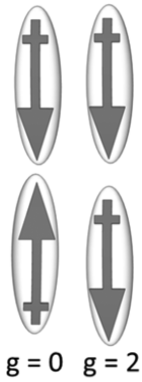

Figure 1. Cartoon depiction of the relative alignment of two polar, rodlike molecules for Kirkwood factors of 0 and 2.

biphenyls, is accounted for through the formation of antiparallel correlated pairs, the concentration and lifetime of which increase with decreasing temperature.[18−21] At a particular concentration, the population of dimers relative to monomers is sufficient to allow the formation of a smectic phase. As the temperature decreases further (and the concentration of dimers increases) the dipolar forces that stabilize the layered structure break down, and in their absence the material reverts to a nematic phase,[14] as depicted in Figure 2.

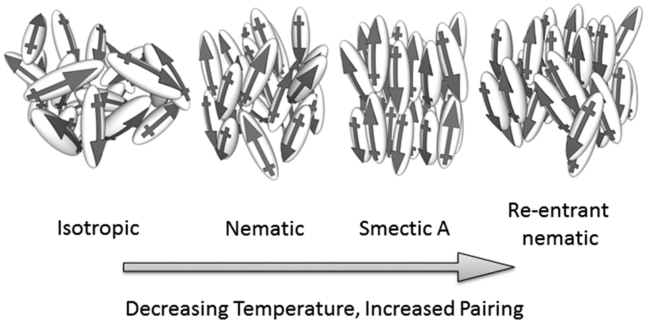

Figure 2. Schematic representation of the antiparallel correlations that lead to re-entrant phase behavior in liquid crystals, as proposed by Cladis.[14]

That highly polar materials tend to align with their dipole moments antiparallel has been demonstrated experimentally via X-ray diffraction studies on 8CB (4-octyl-4′-cyanobiphenyl),[18,22] which reveal that the layer spacing in the smectic A phase is 1.4 times the molecular length, rather than approximately one molecular length, as might be expected. This larger layer spacing is a consequence of antiparallel molecular associations, with the smectic A phase being composed of a mixture of both antiparallel correlated species and individual molecules.

Given that re-entrant phenomena are often a consequence of antiparallel correlations (and the steric constraints these impart), it is surprising to find that Maier−Meier and Kirkwood analysis has not been applied to this problem. For example, the degree and strength of intermolecular associations, and thus the occurrence of re-entrant phenomena, are intimately related to the magnitude of the molecular dipole moment. However, any polar group that serves to disrupt the antiparallel correlations through polar or steric interference (such as F or SCN) will not yield re-entrant behavior. The nitro group has a dipole moment comparable to, and in some cases slightly larger than, that of nitrile. The possibility that mixtures of compounds from the 4-alkoxy-4′-nitrobiphenyl series may exhibit re-entrant polymorphisms has not been explored.

From calculated dipole and polarizability data it is possible to obtain solutions to the Maier−Meier equations that match measured dielectric anisotropy, in effect yielding the Kirkwood factor and thus a qualitative estimate of the degree of antiparallel correlations. We combined this approach with mixture studies and X-ray diffraction to investigate if antiparallel correlated pairs form in two members of the 4-alkoxy-4′-nitrobiphenyl family (i.e., 4-hexyloxy-4′-nitrobiphenyl, **1**, and 4-octyloxy-4′-nitrobiphenyl, **2**), and to probe the incidence and absence of re-entrant behavior in this system and mixtures with 6OCB and 8OCB.

2. RESULTS AND DISCUSSION

2.1. Synthesis. The synthetic pathway to the nitro family of materials is shown in Scheme 1.

Scheme 1

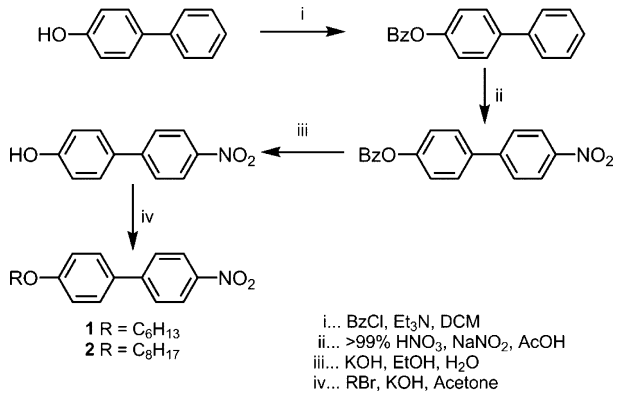

4′-Hydroxy-4-nitrobiphenyl was prepared in 3 steps via the method described by Jones et al., in an overall yield of 48%.[23] 4′-Hydroxy-4-nitrobiphenyl was then alkylated with either 1-bromohexane or 1-bromooctane to give compounds **1** and **2**, respectively. Both compounds were isolated by flash chromatography using silica gel, passed through a short plug of alumina to remove ionic impurities, and recrystallized from hexane, yielding compounds **1** and **2** as pale yellow needles. Detailed synthetic procedures and analytical data are provided in the Supporting Information.

2.2. Mesomorphic Properties. The transition temperatures and associated enthalpies of the compounds prepared for this study were determined via a combination of polarized optical microscopy (POM) and differential scanning calorimetry (DSC) and are presented in Table 1, alongside the thermal behavior of 6OCB and 8OCB for comparison.

The transition temperatures for compounds **1** and **2** are in good agreement with literature values.[26] Although the polymorphism exhibited by the 4-alkoxy-4′-nitrobiphenyl compounds is identical to that of their cyano analogues, 6OCB and 8OCB, the transition temperatures and clearing points are significantly lower. The small measured value for the enthalpy of transition for the nematic to smectic A transition in **2** indicates that the smectic A phase is perhaps quite disordered. The incidence of the smectic A phase in the longer chain homologues of the *n*OCB series is known to be due to the formation of dynamic antiparallel molecular pairing; thus, the observation of a smectic A phase in compound **2** is taken to

DOI: 10.1021/jp512093j
J. Phys. Chem. B 2015, 119, 3273−3280

Table 1. Transition Temperatures (°C) and Associated Enthalpies of Transition (kJ mol^{-1}) for Compounds 1, 2, 6OCB, and 8OCB[24,25]

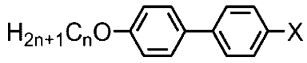

no.	n	X	Cr		SmA		N		Iso
1	6	NO_2	●	67.6 [24.6]	–	–	(●	35.0) [0.2]	●
6OCB	6	CN	●	58.0 [29.0]	–	–	●	75.5 [0.4]	●
2	8	NO_2	●	49.2 [31.5]	●	50.2 [0.1]	●	52.6 [0.3]	●
8OCB	8	CN	●	54.5 [31.2]	●	67.2 [0.1]	●	81.0 [0.7]	●

indicate that a similar phenomenon occurs in the 4-alkoxy-4′-nitrobiphenyl family. However, the extent to which these antiparallel associations form and their lifetime are anticipated to be significantly different from those of the cyano analogues, as inferred by the reduced thermal stability of the mesomorphic state for compounds **1** and **2** relative to their cyano analogues. The layer spacing in the smectic A phase of **2** was measured to be 29.5 Å by small-angle X-ray scattering. This layer spacing is equal to 1.39 times the molecular length (as calculated on geometry minimized at the B3LYP/6-31G(2d,2p) level of theory using extended, all *trans* alkoxy chains), indicating that the smectic A phase is of the subtype SmA_D and implying that the nitrobiphenyl core does give rise to antiparallel correlated species in the same manner as cyanobiphenyl. For comparison, the layer spacing in the smectic A phase 8OCB was found to be temperature invariant and measured to be 31.3 Å, which equates to 1.45 times the molecular length (as calculated on geometry minimized at the B3LYP/6-31G(2d,2p) level of theory). The layer spacing in 8OCB is almost 5% larger than that measured in compound **2** despite the molecular lengths being virtually identical (21.2 Å for **2** and 21.6 Å for 8OCB).

As shown in the diffraction patterns in Figure 3, no higher-order peaks were observed, confirming that the smectic A phase

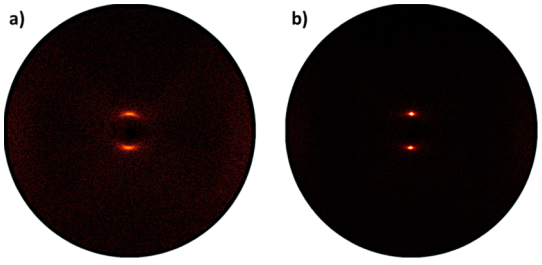

Figure 3. Small-angle X-ray diffraction patterns for the nematic phase (left panel, 51 °C) and smectic A phase (right panel, 45 °C) of compound **2**.

is only weakly ordered. Even with relatively long exposure times (6 min) it was not possible to observe even a second-order peak.

2.3. Mixture Studies. Because the re-entrant phase behavior for the 6OCB/8OCB occurred in the phase diagram at concentrations of 20−30 wt % 6OCB, a similar approach was attempted for mixtures of compounds **1** and **2**. The phase diagram is presented in Figure 4. In addition to the nitro and cyano mixtures, all possible binary combinations of **1**, **2**, 6OCB, and 8OCB were investigated to determine if re-entrancy could

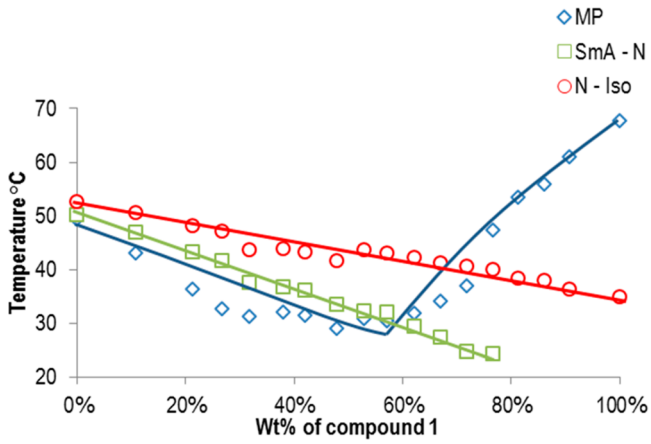

Figure 4. Gibbs phase diagram for binary mixtures (wt %) of compounds **1**/**2** as a function of temperature (°C).

occur between different species. The phase diagrams for these binary mixtures are presented in Figures 5−8.

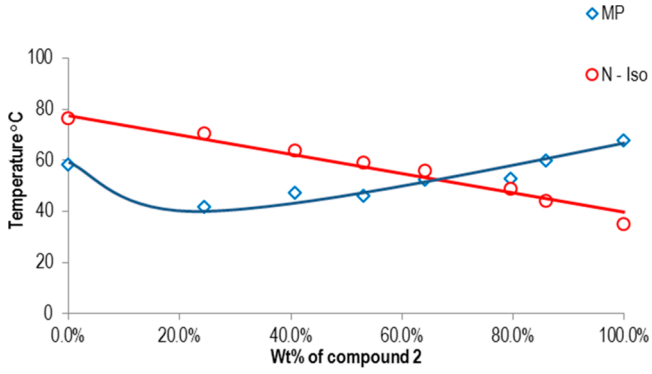

Figure 5. Gibbs phase diagram for binary mixtures (wt %) of 6OCB/**1** as a function of temperature (°C).

In the Gibbs phase diagram between **1** and **2**, the nematic-to-liquid and smectic A-to-nematic phase transition temperatures were observed to vary linearly across the phase diagram; hoowever, at >81 wt % of compound **1**, only the nematic phase is observed; above 72 wt %, the nematic phase is monotropic. By using the measured enthalpies of fusion and melting points for **1** and **2**, it is possible to predict the composition and thermal behavior of the eutectic mixture through the Schröder−van Laar equation.

DOI: 10.1021/jp512093j
J. Phys. Chem. B 2015, 119, 3273−3280

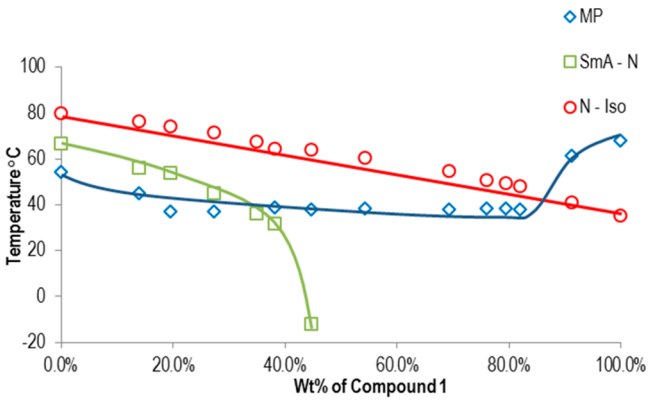

Figure 6. Gibbs phase diagram for binary mixtures (wt %) of 8OCB/**1** as a function of temperature (°C).

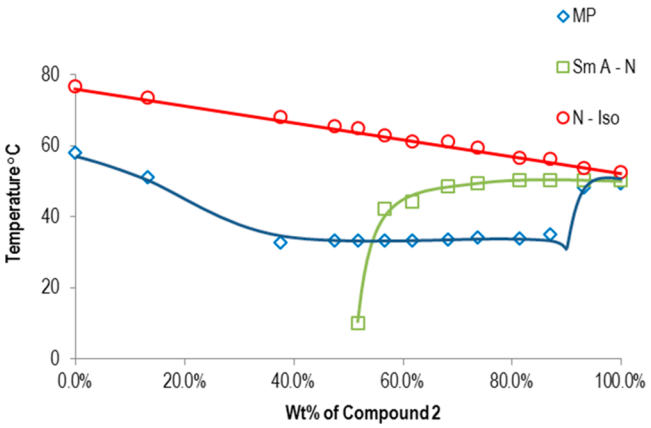

Figure 7. Gibbs phase diagram for binary mixtures (wt %) of 6OCB/**2** as a function of temperature (°C).

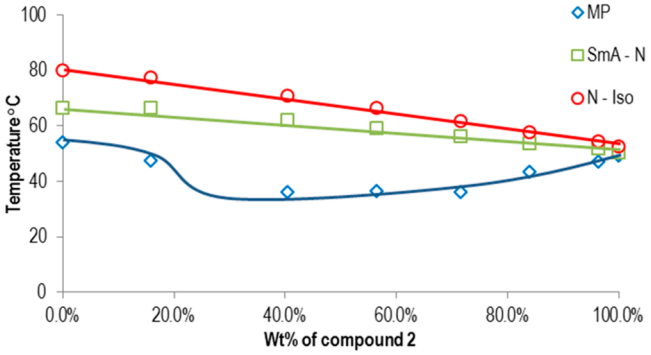

Figure 8. Gibbs phase diagram for binary mixtures (wt %) of 8OCB/**2** as a function of temperature (°C).

In the case of the analogous cyano mixtures, compositions containing between 20% and 30% 6OCB show the phase sequence N−SmA−N_{re}; however, this polymorphism is not observed for mixtures of compounds **1** and **2**. The existence of antiparallel associated dimers is a prerequisite for the formation of smectic phases in cyanobiphenyls; therefore, as discussed previously, it is reasonable to expect that dimerization also occurs and drives the formation of the smectic A phase in nitrobiphenyl compounds. As the smectic A phase persists over a wider range of concentrations for binary mixtures of **1**/**2** than for 6OCB/8OCB, it is reasonable to propose that the associative forces between nitro compounds are stronger than those for the analogous cyano compounds.

Neither 6OCB nor compound **1** exhibits a smectic A phase, and the nematic phase is observed to vary linearly across the phase diagram (Figure 5). Neat 8OCB has a smectic A phase, and this persists across the phase diagram with compound **1** until approximately 45 wt % of **1**, where it is observed to be rapidly suppressed (Figure 6). Similar observations are made for the mixture of compound **2** with 6OCB (Figure 7). It is interesting to note that the smectic A phase persists in these mixtures over a concentration range that is wider than that observed for 6OCB/8OCB. For mixtures of compound **2** with 8OCB, see Figure 8, as both exhibit nematic and smectic A phases, they persist over the entire concentration range of the Gibbs phase diagram. Because there is no observation of re-entrancy and the fact that the smectic A phase is observed over a wider range of concentrations for all these mixture studies, it seems probable that the attractive forces that lead to the formation of antiparallel correlated pairs are stronger for nitro compounds than for cyano compounds.

To explore this hypothesis further, a phase diagram was constructed by mixing compound **1** with the eutectic mixture of 6OCB and 8OCB, which exhibits a re-entrant nematic phase and occurs with 25 wt % of 6OCB. If the degree of antiparallel correlated pairs were smaller for the nitrobiphenyl system than the cyanobiphenyl system this would be expected to lead to a reduction in the smectic A to re-entrant nematic transition temperature, as the concentration of paired species would be lower at a given temperature. As shown in the phase diagram in Figure 9, this is not the case; the smectic A-to-re-entrant nematic transition temperature is almost invariant with concentration and is not observed at greater than 7% of compound **1**, at which point the mixtures no longer exhibit the smectic A phase. Furthermore, the smectic A phase diminishes rapidly with increasing concentration of **1**, which could be attributed to an increased degree of antiparallel association at a given temperature with respect to the parent mixture of 6OCB and 8OCB.

2.4. Dielectric Measurements and Maier−Meier Analysis. To test this hypothesis, Kirkwood factors were estimated from a combination of calculated molecular parameters and measured values of the dielectric anisotropy ($\Delta\varepsilon$) for compounds **1** and **2**, as well as for 6OCB and 8OCB. As the measurement of $\Delta\varepsilon$ is trivial, the success of this method depends on the accuracy of the computed polarizability tensors (α_{xx}, α_{yy}, and α_{zz}) and dipole moment vectors (μ_x, μ_y, and μ_z). In ascertaining the accuracy of the calculated values, polarizabilities and dipole moments determined via a range of computational methods were screened using 5CB as a model compound, for which measured values already exist.

Values of the perpendicular and parallel capacitances ($C_\perp$ and $C_\parallel$, respectively) were measured via the one-cell method[27−29] using an Instec ALCT property tester. The dielectric anisotropy was obtained from a plot of capacitance as a function of voltage, as shown in Figure 10, with the perpendicular capacitance being the average of capacitance at voltages lower than the Fréedericksz transition and the parallel capacitance being that as it approaches saturation. Full details are presented in the Supporting Information.

From the measured values of $C_\perp$ and $C_\parallel$, the dielectric anisotropy ($\Delta\varepsilon$) for 5CB was determined to be 13.2, with an order parameter (S) of 0.60, in agreement with literature values.[30] Using values for molecular polarizability and dipole

DOI: 10.1021/jp512093j
J. Phys. Chem. B 2015, 119, 3273−3280

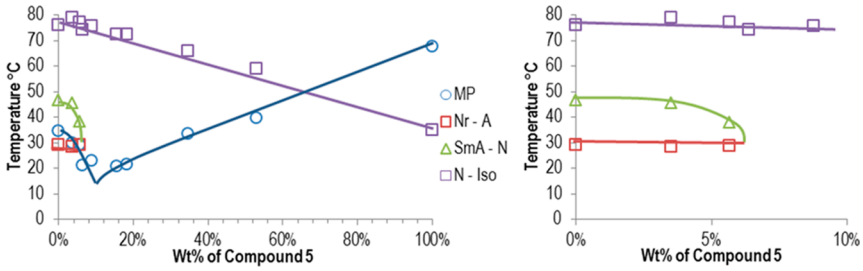

Figure 9. Gibbs phase diagram for ternary mixtures (wt %) of the re-entrant eutectic mixture of 6OCB/8OCB (25 and 75 wt %, respectively) with compound **1** as a function of temperature (°C), left panel, and an expansion of the 0−10% concentration region, with the melting point line omitted for clarity (right panel).

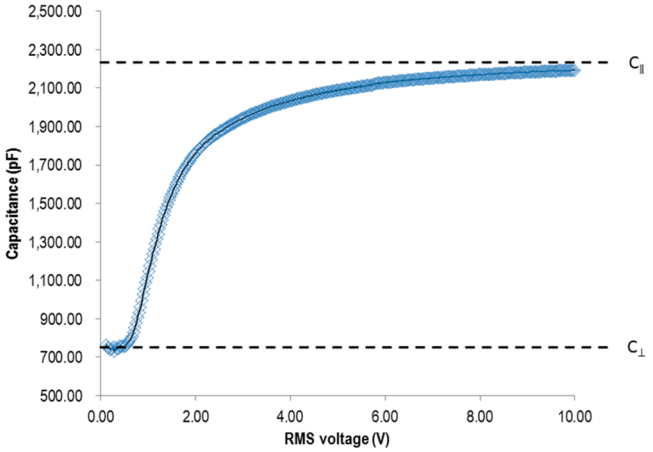

Figure 10. Plot of capacitance (picofarads) as a function of RMS voltage (volts) with a triangular waveform and frequency of 0.5 Hz for 5CB. A double exponential fit is used to extrapolate to $1/V = 0$ to obtain parallel capacitance.

moments calculated by a variety of semiempirical methods, solutions to the Maier−Meier equations were found via variations to the Kirkwood factor (g) so as to reproduce the measured value of $\Delta\varepsilon$ and S, as shown in Table 2.

None of the methods screened can satisfactorily reproduce measured values of molecular dipole moment and polarizability. As the deviation of the computed dipole moments from experimental values is systematic for a given method, this error is included in the Kirkwood factor. Polarizability however is not treated by such a factor, and in order to obtain meaningful values the computed values must be as close as possible to experimental ones. Irrespective of the basis set used, none of the Hartree−Fock, DFT(B3LYP), and MP2 methods screened could satisfactorily reproduce either mean or anisotropic polarizability values. Semiempirical calculations with AM1 and PM7 both produce reasonable polarizability values; however, because PM7 was found to significantly overestimate dipole moments, AM1 was chosen for computation of the molecular properties of **1**, **2**, 6OCB, and 8OCB.[9,37]

The dielectric anisotropies of **1**, **2**, 6OCB, and 8OCB were determined via extrapolation with E7 as a host, with the target

Table 2. Calculated Molecular Dipole Moments, Dipolar Angles, and Polarizabilities of 5CB at Various Levels of Theory, and Kirkwood Factors (g) Required to Obtain Solutions to the Maier−Meier Equations When $\Delta\varepsilon \approx 13.20$ and $S = 0.60$

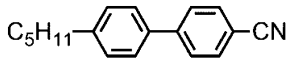

method	μ (D)	β	α_{avg} (Å^3)	$\Delta\alpha$ (Å^3)	$\Delta\varepsilon$	S	g
experimental	4.77[31]	–	33.7[32]	17.6[33]	13.200[a]	0.60[a]	0.54[a]
AM1[b]	4.12	2.07	33.45	14.02	13.197	0.60	0.5280
RM1[b]	4.51	1.89	24.19	23.83	13.201	0.60	0.6630
PM3[b]	4.27	1.75	32.56	24.74	13.201	0.60	0.5320
PM6[b]	5.45	1.79	33.47	21.14	13.203	0.60	0.3043
PM7[b]	5.50	1.71	34.59	19.94	13.199	0.60	0.2984
HF/6-31G[c]	6.06	8.78	28.08	25.68	13.201	0.60	0.2918
HF/6-31G(d)[c]	5.94	5.30	27.34	23.24	13.200	0.60	0.3037
HF/6-31G(d,p)[c]	5.99	8.51	27.95	23.66	13.199	0.60	0.3008
B3LYP/6-31G(d,p)[c]	5.92	8.43	31.01	31.68	13.199	0.60	0.2770
B3LYP/6-31G(2d,p)[c]	5.98	8.34	34.67	31.68	13.188	0.60	0.2570
B3LYP/6-311++G(2d,2p)[c]	6.81	7.09	35.39	32.49	13.205	0.60	0.2008
MP2/6-31G[d]	6.02	8.81	27.58	23.54	13.208	0.60	0.3020
MP2/6-31G(d)[d]	6.03	8.95	28.49	25.09	13.199	0.60	0.2926
MP2/6-31G(d,p)[d]	6.01	8.90	28.92	25.89	13.208	0.60	0.2866
MP2/6-311++G(2d,2p)[d]	6.27	8.01	31.22	27.59	13.203	0.60	0.2471

[a]Values of $\Delta\varepsilon$ and S were measured as described in the text, yielding a g factor value of 0.54. [b]Semiempirical calculation performed in MOPAC 2012.[34] [c]Calculation performed in GAMESS-UK.[35] [d]Calculation performed in Gaussian 09.[36]

DOI: 10.1021/jp512093j
J. Phys. Chem. B 2015, 119, 3273−3280

Table 3. Comparison of the Dielectric Anisotropy ($\Delta\varepsilon$) of 6OCB, 8OCB, 1, and 2 Extrapolated from Mixtures with E7[a]

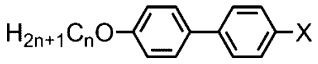

no.	n	X	$\Delta\varepsilon$	μ (D)	$\Delta\alpha$ (Å^3)	$g_{S=0.4}$	$g_{S=0.5}$	$g_{S=0.6}$	$g_{S=0.7}$
1	6	NO_2	8.79	6.992	15.29	0.227	0.180	0.148	0.126
6OCB	6	CN	10.85	4.686	16.44	0.624	0.495	0.408	0.375
2	8	NO_2	8.70	7.049	15.74	0.248	0.1962	0.1619	0.1375
8OCB	8	CN	10.88	4.678	17.33	0.675	0.536	0.443	0.376

[a]Net dipole moments (μ) and polarizability ($\Delta\alpha$) were computed semiempirically with the AM1 hamiltonian. Kirkwood factors (g) were obtained as described in the text and are given for order parameters (S) of 0.4, 0.5, 0.6, and 0.7.

material in a concentration of approximately 30 wt %. From the measured dielectric anisotropy of the host, the mole fraction (x) and the measured dielectric anisotropy for the solution the dielectric anisotropy of the neat material was obtained via eq 5.[6]

$$\Delta\varepsilon = (1 - x)\Delta\varepsilon_{\text{host}} + x\Delta\varepsilon_{\text{measured}} \quad (5)$$

For **1**, **2**, 6OCB, and 8OCB, dipole and polarizability data was calculated using the AM1 Hamiltonian (MOPAC2012)[34] on geometry minimized using the B3LYP functional and the 6-311++G(2d,2p) basis set (Gaussian 09).[36] Solutions to the Maier–Meier equations were obtained for order parameters of 0.4, 0.5, 0.6, and 0.7 via adjustment of the Kirkwood factor so that the calculated value of $\Delta\varepsilon$ matched the extrapolated value. The calculated dipole moments, anisotropic polarizabilities, and Kirkwood factors are presented in Table 3.

Calculated dipole moments for **1** and **2** are significantly larger than those of the analogous cyano compounds, and although the computed polarizability is only slightly smaller, this leads to smaller values of dielectric anisotropy. When both the Kirkwood factor and order parameter used when obtaining solutions to the Maier–Meier equation are adjusted, it is possible to match the calculated values of dielectric anisotropy with those measured experimentally. As the order parameter is not known, a range of reasonable values (0.4–0.7) was used; back-calculation gave the Kirkwood factors presented in Table 3 and plotted as a function of the order parameter in Figure 11.

For a given order parameter, the calculated Kirkwood factors for compounds **1** and **2** are smaller than those for 6OCB and 8OCB, implying that the degree of antiparallel correlations for the nitro materials is greater than that for their cyano counterparts. This study complements the observations made in binary mixtures and also leads us to the conclusion that the associative forces for nitrobiphenyl are stronger than those for cyanobiphenyl derived materials. Furthermore, this analysis of the Kirkwood factors implies that the nematic phase of the nitrobiphenyl materials is composed primarily of antiparallel correlated pairs, similar to the re-entrant nematic of the cyanobiphenyls. That said, the difference in Kirkwood factors between the nitro- and cyano- systems could possibly arise because of different packing arrangements in these materials.

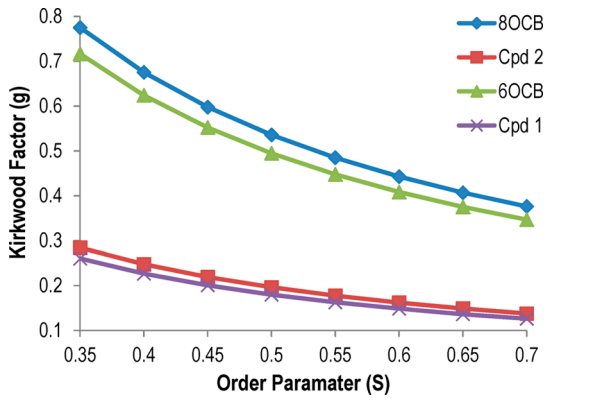

Figure 11. Plot of Kirkwood factor (g) versus the order parameter (S) as used in the Maier–Meier equations to yield a value of $\Delta\varepsilon$ equal to that given in Table 3 for compounds **1**, **2**, 6OCB, and 8OCB.

3. CONCLUSIONS

Given the similar polarity and polarizability of 4-alkoxy-4′-nitrobiphenyl and 4-alkoxy-4′-cyanobiphenyl certain concentrations, the phase diagram for the analogous nitro-terminated materials does not exhibit any re-entrant phenomena. The absence of re-entrant behavior was examined through Gibbs phase diagrams for mixed cyano/nitro biphenyl systems. In the 6OCB/8OCB phase diagram, the smectic A phase exists because of the presence of unpaired molecules; hence, there is a lack of stabilization of the smectic A phase in mixture studies with nitro compounds. It was hypothesized that re-entrant behavior is not observed because of *increased* strength of intermolecular quadrupolar interactions for nitro systems compared to cyano systems. By calculating the dielectric anisotropy of **1**, **2**, 6OCB, and 8OCB (through the Maier–Meier equations using dipole and polarizability data computed semiempirically using the AM1 Hamiltonian) and by comparing this to measured values, it was possible to obtain values of the Kirkwood factor as a function of the order parameter for each material. The Kirkwood factor for **1** and **2** is lower than that obtained for 6OCB and 8OCB for a given order parameter, indicating that the "effective molecular dipole moment" is reduced because of the presence of significant antiparallel correlations. This indicates that the degree of antiparallel association for the nitro systems is greater than that for their cyano analogues. Although applied to only the 6OCB/8OCB and 6ONO$_2$B/8ONO$_2$B (**1** and **2**, respectively) systems, this combined experimental and computational analytical method could be applied to other re-entrant systems, especially those in which nitro-terminated materials are re-entrant but their cyano analogues are not, such as DB9ONO$_2$ and DB9OCN.[38−41]

■ ASSOCIATED CONTENT

Supporting Information

Details of the measurement of dielectric anisotropy and experimental methods used; synthetic details; and analytical data for compounds **1**, **2**, and intermediate materials. This material is available free of charge via the Internet at http://pubs.acs.org.

DOI: 10.1021/jp512093j
J. Phys. Chem. B 2015, 119, 3273−3280

AUTHOR INFORMATION

Corresponding Author

*E-mail: Richard.mandle@york.ac.uk. Tel.: +441904 432539.

Notes

The authors declare no competing financial interest.

ACKNOWLEDGMENTS

R.J.M. thanks the UK MOD, QinetiQ, and the EPSRC for award of an industrial CASE studentship.

REFERENCES

(1) Maier, W.; Meier, G. A Simple Theory of the Dielectric Characteristics of Homogenously Orientated Liquid-Crystalline Phases of the Nematic Type. *Z. Naturforsch., A: Astrophys., Phys. Phys. Chem.* **1961**, *16A*, 262−267.

(2) Onsager, L. Electric Moments of Molecules in Liquids. *J. Am. Chem. Soc.* **1936**, *58*, 1486−1493.

(3) Urban, S. In *Physical Properties of Liquid Crystals: Nematics*; Dunmur, D. A., Fukuda, A., Luckhurst, G. R., Eds.; IEE: London, 2001; pp 267−276.

(4) Dunmur, D., Toriyama, K. In *Handbook of Liquid Crystals*; Demus, D., Goodby, J. W., Gray, G. W., Spiess, H.-W., Vill, V., Eds.; Wiley-VCH: Weinheim, Germany, 1998; Vol. *1*, pp 231−252.

(5) Januszko, A.; Glab, K. L.; Kaszynski, P.; Patel, K.; Lewis, R. A.; Mehl, G. H.; Wand, M. D. The Effect of Carborane, Bicyclo[2.2.2]-octane and Benzene on Mesogenic and Dielectric Properties of Laterally Fluorinated Three Ring Mesogens. *J. Mater. Chem.* **2002**, *16*, 3183−3192.

(6) Ringstrand, B.; Kaszynski, P.; Januszko, A.; Young, V. G. Polar Derivatives of the $[closo\text{-}1\text{-}CB_9H_{10}]^-$ Cluster as Positive $\Delta\varepsilon$ Additives to Nematic Hosts. *J. Mater. Chem.* **2009**, *19*, 9204−9212.

(7) Ran, Z.; Jun, H.; Zheng-Hui, P.; Li, X. Calculating the Dielectric Anisotropy of Nematic Liquid Crystals: A Reinvestigation of the Maier-Meier Theory. *Chin. Phys. B* **2009**, *18*, 2885−2892.

(8) Kaszynski, P.; Januszko, A.; Glab, K. L. Comparative Analysis of Fluorine-Containing Mesogenic Derivatives of Carborane, Bicyclo[2.2.2]octane, Cyclohexane and Benzene Using the Maier-Meier Theory. *J. Phys. Chem. B* **2014**, *118*, 2238−2248.

(9) Demus, D.; Inukai, T. Calculation of Molecular, Dielectric and Optical Properties of 4′-*n*-pentyl-4-cyano-biphenyl (5CB). *Liq. Cryst.* **1999**, *26*, 1257−1266.

(10) Kirkwood, J. G. The Dielectric Polarisation of Polar Liquids. *J. Chem. Phys.* **1939**, *7*, 911−919.

(11) Bordewijk, P. Extension of the Kirkwood-Frölich Theory of the Static Dielectric Permittivity to Anisotropic Liquids. *Physica (Amsterdam)* **1974**, *75*, 146−156.

(12) Prestbo, E. W.; McHale, J. L. Static Dielectric Constants and Kirkwood Correlations Factors of Dimethyl Sulfoxide/Carbon Tetrachloride Solutions. *J. Chem. Eng. Data* **1984**, *29*, 387−389.

(13) Ringstrand, B.; Kaszynski, P. High $\Delta\varepsilon$ Nematic Liquid Crystals: Fluxional Zwitterions of the $[closo\text{-}1\text{-}C_9B_{10}]^-$ Cluster. *J. Mater. Chem.* **2011**, *21*, 90−95.

(14) Cladis, P. E. New Liquid Crystal Phase Diagram. *Phys. Rev. Lett.* **1971**, *35*, 48−51.

(15) Cladis, P. E.; Mandle, R. J.; Goodby, J. W. Reentrant Phase Transitions in Liquid Crystals. In *The Handbook of Liquid Crystals*, 2nd ed; Goodby, J. W., Collings, P. J., Kato, T., Tschierske, C., Gleeson, H., Raynes, E. P., Eds.; Wiley-VCH: Weinheim, Germany, 2014.

(16) Riblet, G.; Winzer, K. Vanishing of Superconductivity Below a Second Transition Temperature in $(La_{1-\chi}Ce_\chi)Al_2$ Alloys Due to the Kondo Effect. *Solid State Commun.* **1971**, *9*, 1663−1665.

(17) Cladis, P. E.; Guillon, D.; Bouchet, F. R.; Flinn, P. L. Reentrant Nematic Transitions in Cyanooctyloxybiphenyl. *Phys. Rev. A: At., Mol., Opt. Phys.* **1981**, *23*, 2594−2601.

(18) Gray, G. W.; Lydon, J. E. New Type of Smectic Mesophase? *Nature* **1974**, *252*, 221−222.

(19) Cladis, P. E.; Bogardus, R. K.; Aadsen, D. High Pressure Investigation of the Reentrant Nematic Bilayer Smectic-A Transition. *Phys. Rev. A: At., Mol., Opt. Phys.* **1979**, *18*, 2292−2306.

(20) Hafiz, N.; Vaz, N. A. P.; Yaniv, Z.; Allender, D.; Doane, J. W. ^{2}D NMR Observation of Pairing in Materials Forming the Reentrant Nematic Phase. *Phys. Lett. A* **1982**, *91*, 411−413.

(21) Indekeu, J. O.; Berker, A. N. Quadruple Reentrance (Nematic−Smectic-A_d−Nematic−Smectic-A_d−Nematic−Smectic-A_1) from the Frustrated Spin-Gas Model of Liquid Crystals. *Phys. Rev.* **1982**, *33A*, 1158−1162.

(22) Leadbetter, A. J.; Frost, J. C.; Gaughan, J. P.; Gray, G. W.; Mosely, A. The Structure of Smectic A Phases of Compounds with Cyano End Groups. *J. Phys. (Paris)* **1979**, *40*, 375−380.

(23) Jones, B.; Chapman, F. The Nitration of Esters of 4-Hydroxydiphenyl. The Preparation of 4-Hydroxy-4′- and -2′-Nitro-diphenyls. *J. Chem. Soc.* **1952**, 1829−1832.

(24) Itahara, T.; Tamura, H. Comparison of Liquid Crystalline Properties of Symmetric and Nonsymmetric Liquid Crystal Trimers. *Mol. Cryst. Liq. Cryst.* **2007**, *474*, 17−27.

(25) Mouquino, A.; Saavedra, M.; Maiau, A.; Petrova, K.; Barros, M. T.; Figuerinhas, J. L.; Sotomayor, J. Films Based on New Methacrylate Monomers: Synthesis, Characterisation and Electrooptical Properties. *Mol. Cryst. Liq. Cryst.* **2011**, *542*, 557−566.

(26) Gray, G. W.; Harrison, K. J.; Nash, J. A.; Constant, J.; Hulme, D. S.; Kirton, J.; Raynes, E. P. Stable, Low Melting Nematogens of Positive Dielectric Anisotropy for Display Devices. In *Liquid Crystals and Ordered Fluids*; Johnson, J. F., Porter, R. S., Eds.; Plenum Press: London, 1973; pp 617−643.

(27) Clark, M. G.; Raynes, E. P.; Smith, R. A.; Tough, R. J. A. Measurement of the Permittivity of Nematic Liquid Crystals in Magnetic and Electric Fields Using Extrapolation Procedures. *J. Phys. D: Appl. Phys.* **1980**, *13*, 2151−2156.

(28) Wu, S. T.; Coates, D.; Bartmann, E. Physical Properties of Chlorinated Liquid Crystals. *Liq. Cryst.* **1991**, *10*, 635−646.

(29) Murakami, S.; Naito, H. Electrode and Interfacial Polarisation in Nematic Liquid Crystal Cells. *Jpn. J. Appl. Phys.* **1997**, *36*, 2222−2225.

(30) Goodby, J. W.; Davis, E. J.; Mandle, R. J.; Cowling, S. J. Nano-Segregation and Directed Self Assembly in the Formation of Functional Liquid Crystals. *Isr. J. Chem.* **2012**, *52*, 863−880.

(31) Kedziora, P.; Jadzyn, J.; Bonnet, P. Dielectric Studies of the Association of Strongly Polar Molecules. *Ber. Bunsen-Ges.* **1993**, *97*, 864−867.

(32) Urban, S.; Kędzierski, J.; Dąbrowski, R. Analysis of the Dielectric Anisotropy of Typical Nematics with the Aid of the Maier-Meier Equations. *Z. Naturforsch.* **2000**, *55A*, 449−456.

(33) Urban, S. Comparison of the Dielectric Properties of 4-(2-Methylbutyl)-4′-cyanobiphenyl (5*CB) and 4-Pentyl-4′-cyanobiphenyl (5CB) in the Liquid State. *Phys. Chem. Chem. Phys.* **1999**, *1*, 4843−4846.

(34) Stewart, J. J. P. *MOPAC2012*. Stewart Computational Chemistry: Colorado Springs, CO, 2012; HTTP://OpenMOPAC.net.

(35) Guest, M. F.; Bush, I. J.; van Dam, H. J. J.; Sherwood, P.; Thomas, J. M. H.; van Lenthe, J. H.; Havenith, R. W. A.; Kendrick, J. The GAMESS-UK Electronic Structure Package: Algorithms, Developments and Applications. *Mol. Phys.* **2001**, *103*, 719−747.

(36) Frisch, M. J.; Trucks, G. W.; Schlegel, H. B.; Scuseria, G. E.; Robb, M. A.; Cheeseman, J. R.; Scalmani, G.; Barone, V.; Mennucci, B.; Petersson, G. A.; et al. *Gaussian 09*, revision D.01; Gaussian, Inc.: Wallingford, CT, 2009.

(37) Stewart, J. J. P. Optimization of Parameters for Semiempirical Methods VI: More Modifications to the NDDO Approximations and Re-optimization of Parameters. *J. Mol. Model.* **2013**, *19*, 1−32.

(38) Tinh, N. H.; Hardouin, F.; Destrade, C. Trois Phénomènes Rentrants Dans un Produit pur Mésogène. *J. Phys. (Paris)* **1982**, *43*, 1127−1131.

(39) Shashidhar, R.; Ratna, B. R.; Surendranath, V.; Raja, V. N.; Krishna Prasad, S.; Nagabhushan, C. Experimental Studies on a Triply Reentrant Mesogen. *J. Phys., Lett.* **1985**, *46*, 445−450.

DOI: 10.1021/jp512093j
J. Phys. Chem. B 2015, 119, 3273−3280

(40) Tinh, N. H.; Hardouin, F.; Destrade, C.; Gasparoux, H. New Phase Transitions in S_C-S_{C_2} and S_{A_d}-S_{C_2} in Pure Mesogens. *J. Phys., Lett.* **1982**, *43*, 739−744.
(41) Fontes, E.; Heiney, P. A.; Haseltine, J. L.; Smith, A. B. High Resolution X-Ray Scattering Study of the Multiply Reentrant Polar Mesogen DB_9ONO_2. *J. Phys. (Paris)* **1986**, *47*, 1533−1539.

DOI: 10.1021/jp512093j
J. Phys. Chem. B 2015, 119, 3273−3280